

PAPER • OPEN ACCESS

## An approach to define the minimum detectable damage and the alarm thresholds in vibration-based SHM systems

To cite this article: Soroosh Kamali *et al* 2024 *J. Phys.: Conf. Ser.* **2647** 182008

View the [article online](#) for updates and enhancements.

### You may also like

- [Vibration Effect on Natural Convection Heat Transfer in an Inclosed Cubic Cavity](#)  
Baydaa Khalil Khudhair, Adel Mahmood Salh and Ali Ekaid
- [Zeeman-Birefringence He-Ne Dual Frequency Lasers](#)  
Jin Yu-Ye, Zhang Shu-Lian, Li Yan et al.
- [About the calculus of the relative frequency shifts for a beam with multiple cracks](#)  
G R Gillich, D Nedelcu, C O Hamat et al.



The Electrochemical Society

Advancing solid state & electrochemical science & technology

**DISCOVER**  
how sustainability  
intersects with  
electrochemistry & solid  
state science research



# An approach to define the minimum detectable damage and the alarm thresholds in vibration-based SHM systems

Soroosh Kamali<sup>1,2</sup>, Said Quqa<sup>1</sup>, Antonio Palermo<sup>1</sup> and Alessandro Marzani<sup>1</sup>

<sup>1</sup> Department of Civil, Chemical, Environmental and Materials Engineering, University of Bologna, Bologna, Italy

<sup>2</sup> Department of Civil and Environmental Engineering, Shiraz University of Technology, Shiraz, Iran

E-mail: soroosh.kamali2@unibo.it, said.quqa2@unibo.it, antonio.palermo6@unibo.it, alessandro.marzani@unibo.it

**Abstract.** This paper proposes an approach to defining the alarm thresholds for vibration-based structural health monitoring (SHM). The approach uses natural frequencies identified from the acceleration response of the monitored structure and is based on the concept of Minimum Detectable Damage (MDD), namely the smallest damage size in each structural element associated with a given probability of detection (POD) and probability of false alarm (PFA). The approach is demonstrated using natural frequencies computed from finite element models of the healthy and damaged structure, also accounting for temperature fluctuations and measurement noise. The approach first builds a baseline dataset of modal frequencies for a yearly thermal cycle on the healthy structure. Then, different damage conditions are simulated. For each sample of natural frequencies, a Damage Index (DI) is computed as the Mahalanobis distance between the considered sample and the baseline distribution. The alarm threshold is defined as the DI value for a given PFA. Based on the DIs obtained for the damaged structure, the POD is computed for the considered system threshold. This operation is repeated by increasing the damage entity. The MDD is thus defined as the level of damage associated with a desired value of POD. The proposed idea is tested on a steel truss bridge, where the MDD for each element is estimated by considering PFA=5% and POD=95%.

## 1. Introduction

The progressive aging and related deterioration of civil structures and infrastructure is becoming a major concern worldwide and is motivating the spreading of structural health monitoring (SHM) systems aimed at providing a real-time assessment of structural conditions [1].

Among the most effective SHM techniques, those based on structural features derived from vibration responses are particularly appealing due to their ease of implementation [2]. The features collected over the monitoring phase are processed with the objective of identifying changes in their statistical pattern over time, which may indicate structural modifications or potential damages. To achieve this, a scalar parameter, referred to as damage index (DI), is typically computed as a function of the features extracted from the recorded signals and tracked over time [3, 4, 1]. In general, in vibration-based SHM, the features extracted to compute the



DI include modal parameters, namely frequencies, mode shapes, and damping ratios, identified by operational modal analysis (OMA) [2, 5].

Periodic evaluation of the DI allows for assessing the structural state by comparing the DI value with a threshold. If the threshold is exceeded, the SHM system warrants an alarm to warn about the anomalous structural response, which may be related to the insurgence of structural damage. However, in real-world applications, this procedure is not trivial. Civil structures are exposed to different environmental factors, such as varying temperature and humidity, and also unavoidable measurement noise [3, 6, 7, 8, 9]. These factors can affect the calculated DIs and lead to false alarms. Additionally, some damage states may not be detected, especially when their entity is small [10]. Consequently, selecting the appropriate alarm threshold is a trade-off between the number of false alarms and damage detection capabilities of the system [11, 10, 12].

In this paper, we propose a simple strategy to set the alarm threshold and define the smallest damage entity successfully identified by the SHM system. The alarm threshold is set based on the probability of false alarm (PFA). To this purpose, the DIs of the undamaged structure are computed, and the threshold is adjusted such that the probability of exceeding is 5%.

Setting the alarm threshold on the PFA offers several advantages, including enhanced control over the number of false alarms based on the owner's budget and risk tolerance.

For a given threshold, it is fundamental to understand the minimum damage size that the SHM system is capable of detecting with a given probability of damage detection (POD). Thus, a concept called Minimum Detectable Damage (MDD) is herein introduced, which is defined as the minimum damage size that corresponds to a sufficiently large POD. To this purpose, once the alarm threshold has been set based on PFA, for each damage scenario, here simulated numerically, the damage size is increased incrementally, and the related POD is computed. The minimum size providing the desired POD is reported as the MDD for that scenario.

The proposed approach is tested through a numerical example, i.e., a planar steel truss structure. For this example, the DI is calculated using natural frequencies, obtained also considering the effects of temperature variations and measurement noise based on realistic information retrieved from the literature.

## 2. PFA-driven alarm thresholds and MDD

In this section, we describe a classical damage index DI used in SHM, a procedure for the definition of the SHM system alarm threshold, and an algorithm to evaluate the minimum detectable damage (MDD).

### 2.1. Damage index

We consider a damage index (DI) based on the frequencies of vibration. In particular, the frequencies, generally estimated via OMA procedures from the recorded accelerations, are stored in a  $M \times N$  matrix  $\mathbf{HF}$ , where  $N$  is the number of performed OMA instances, and  $M$  is the number of frequencies. We consider the  $N$  instances over a period of time where the structure is supposed to be in its healthy state. This period is generally labeled as the training period and the  $\mathbf{HF}$  matrix as the baseline.

For each instance  $n \in N$ , characterized by the frequencies  $f_n = [f_n^1, f_n^2, \dots, f_n^M]^T$ , we compute a scalar damage index  $DI_n$  using the classical Mahalanobis distance metric [3] as:

$$DI_n = \sqrt{(f_n - \mu[\mathbf{HF}])^T \mathbf{S}^{-1}[\mathbf{HF}](f_n - \mu[\mathbf{HF}])} \quad (1)$$

where  $\mu[\mathbf{HF}] = [\mu^1, \mu^2, \dots, \mu^M]^T$  is the  $1 \times M$  baseline mean value vector and  $\mathbf{S}[\mathbf{HF}]$  the  $M \times M$  baseline covariance matrix. In practice, the Mahalanobis distance is a measure between a sample point, e.g.,  $f_n$ , and a probability distribution  $Q(\vec{\mu}, \mathbf{S})$  in a multi-dimensional space taking into account the correlation of the data set.

As an example, in Fig. 1a we show the DI computed over a two-year period. In the first year (blue dots), the structure is undamaged, and the entire period is used to set the baseline  $[\mathbf{HF}]$  matrix. The DI oscillates as the frequencies vary over time due to environmental variability (e.g., seasonal temperature variations) and measurement noise.

At the beginning of the second year (red dots), the structure is damaged, and the DI is computed for the second year still considering the baseline  $[\mathbf{HF}]$  matrix.

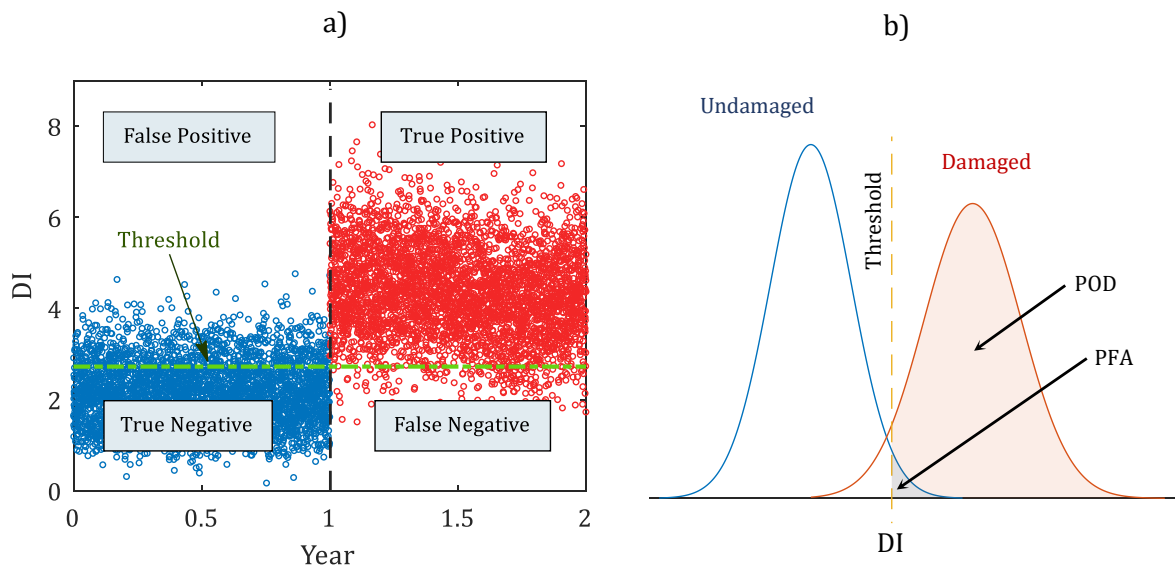


**Figure 1.** Classification based on an alarm threshold: a) different outcomes; b) PFA and POD from the probability density functions.

## 2.2. Alarm threshold

Here we exploit the probability of false alarm  $PFA$  and probability of damage detection  $POD$  to define the alarm threshold for the SHM system and later to estimate the minimum detectable damage.

In particular, out of the DI values of the baseline, we define an alarm threshold  $\tau$ , represented as the green horizontal line in Fig. 1, such that any DI below  $\tau$  is considered as healthy (negative), and any DI above  $\tau$  is considered damaged (positive). For such threshold, the healthy samples with  $DI > \tau$  will be wrongly indicated as false positives  $FP(\tau)$  (see Fig. 1 top-left quarter), whereas all  $DI < \tau$  will be indicated as true negatives  $TN(\tau)$  (see Fig. 1 bottom-left quarter). In this supervised scenario, where damage is known, all the damaged samples with  $DI > \tau$  will be indicated as true positive  $TP(\tau)$  (see Fig. 1 top-right quarter) and all  $DI < \tau$  will be indicated as false negative  $FN(\tau)$  (see Fig. 1 bottom-right quarter).

Thus, for a given  $\tau$  is possible to compute the probability of false alarm  $PFA(\tau)$  and the probability of damage detection  $POD(\tau)$  as:

$$PFA(\tau) = \frac{FP(\tau)}{FP(\tau) + TN(\tau)}, \quad POD(\tau) = \frac{TP(\tau)}{TP(\tau) + FN(\tau)} \quad (2)$$

where the  $PFA(\tau)$ , set on the baseline data, denotes the probability that a DI is above the threshold after the training period for an undamaged scenario, and thus a false alarm is activated, whereas the  $POD(\tau)$  denotes the probability that the DI is actually above the threshold for

a damaged scenario after the training period. The  $PFA(\tau)$  and  $POD(\tau)$  are graphically represented in Fig. 1b on the distributions of the DIs for the healthy and damaged structure.

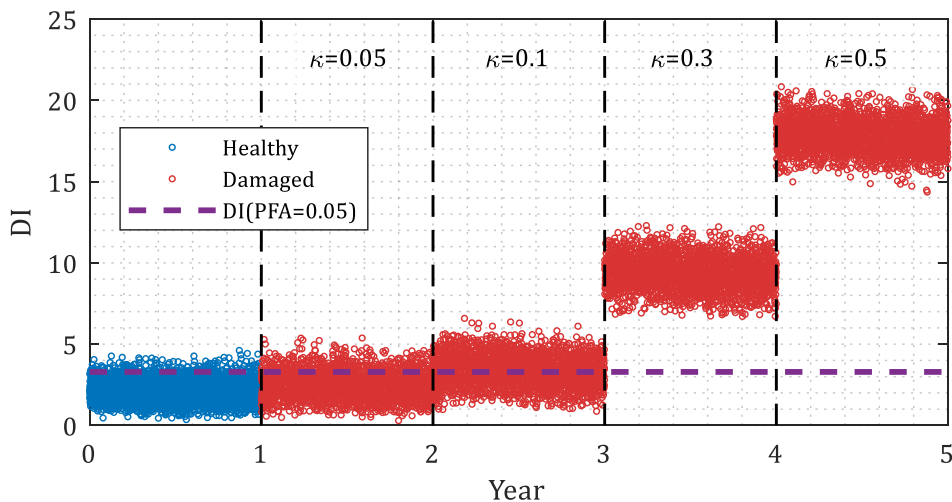


**Figure 2.** DI distributions for the undamaged structure (baseline) in blue and for different damaged structures, namely  $\kappa = 0.05, 0.1, 0.3, 0.5$ , in red.

Fig. 2 shows the DIs for the undamaged structure (baseline) and increasing levels of damage, here denoted by  $\kappa = 0.05, 0.1, 0.3, 0.5$ . For each case, one year of DIs has been simulated.

Note that the SHM alarm threshold  $\tau$  is here taken as  $PFA = 5\%$  and indicated in Fig. 2 as a dashed line. It follows that even if the structure will not experience any damage in the future, at least the 5% of the DIs are expected to be above the threshold. In practice, considering the amount of budget that the structure owner/manager can invest yearly in inspections, the maximum PFA can be set.

### 2.3. Minimum detectable damage

For a given damage level  $\kappa$ , the Receiver Operating Characteristic (ROC) curve, namely the  $POD(\tau)$  vs  $PFA(\tau)$  curve for  $0 \leq \tau \leq \infty$ , can be obtained (see for instance the curve  $\kappa = 0.05$  in Fig. 3). Basically, the ROC curve assesses the quality of the adopted DI in properly classifying the damaged scenario as damaged with respect to a random classifier. For the same damage scenario, a different DI metric yields a different ROC curve. See, for instance, Ref. [13], where it is shown how the number of frequencies  $M$  used to build the DI metric impacts the ROC curve.

Still, for a given number of frequencies  $M$ , it can be observed that by increasing the damage size, the DIs grow, meaning that the  $POD$  vs  $PFA$ , i.e., the ROC, increases as well. For example, for the largest damage size considered in Fig. 3, i.e.  $\kappa = 0.5$ , it can be observed that all the related red dots in Fig. 2 are well above the selected threshold  $PFA = 5\%$  so that the  $POD = 100\%$ . It can also be observed that by varying the PFA from 0 to 100% the  $POD$  would not change. In this case, namely when the ROC curve has  $POD=1$  for any PFA value, the adopted DI is considered a perfect classifier for the related damage scenario.

It follows that the ROC curve can be exploited to "size" the damage for a given adopted DI metric, as it can be easily seen in Fig. 3 where the ROC curves for  $\kappa = 0, 0.05, 0.1, 0.3, 0.5$  are shown. In particular, in this work, we estimate the minimum damage severity that can be detected with  $PFA = 0.05$  and  $POD = 0.95$  as MDD.

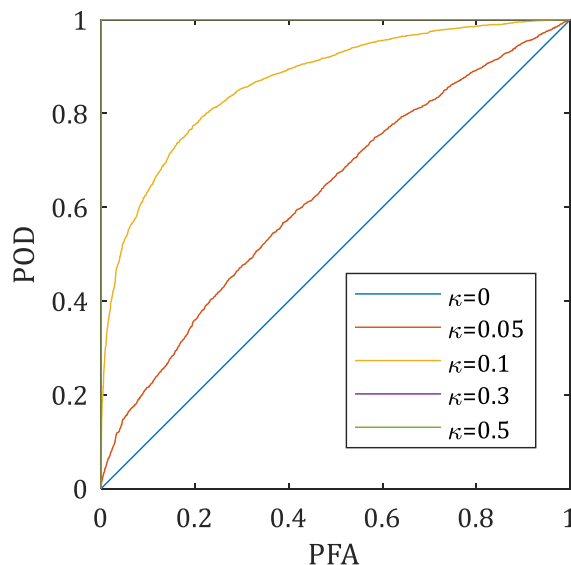


**Figure 3.** Receiver operating characteristic (ROC) curves for different damage sizes ( $\kappa$ ).

#### 2.4. Procedure

Summarizing, the procedure used to estimate the MDD for a given damage is the following:

- (i) the SHM system allows identifying natural frequencies for the undamaged structure (baseline), and the DI is built using the Mahalanobis distance; it is suggested to include in the baseline the DI computed for a period of time in which the structure is exposed to the maximum range of temperature variability (one year); the threshold  $\tau$  is set on the baseline DIs as the one related to  $PFA = 5\%$ ;
- (ii) a reliable model, generally FEM, is prepared to compute the pseudo-frequencies of vibration (i.e., simulated) for the damaged structure; this model should be updated using the frequencies of vibration of the undamaged structure; in view of this step, a set of temperature samples corresponding to one year of fluctuations are generated [14];
- (iii) for a considered damage type  $i$  of interest:
  - (a) a damage size  $\kappa$ , from 0 to 1, is considered, and the damage type  $i$  with size  $\kappa$  is modeled;
  - (b) for each temperature sample, the thermal effect is numerically applied to the model (generally to the modulus of elasticity of some structural elements and/or at the boundary conditions [7]); and the frequencies of vibration are calculated;
  - (c) the computed frequencies are polluted by a zero-mean uniformly distributed noise with a given standard deviation (noise level);
  - (d) the DIs of the damaged samples are calculated as described in Eq. (1) and the  $POD$  for the given  $\tau$  computed;
  - (e) if the  $POD < 0.95$ , the steps (a) to (d) are repeated by increasing the damage size  $\kappa$  until the  $POD$  reaches 0.95.

Following the above procedure, the smallest size of the damage  $i$  that the assumed DI metric can detect for a given  $PFA = 0.05$  and  $POD = 0.95$  is estimated, namely the MDD.

In the next section, we apply the procedure by computing the MDD on a truss structure, considering that only one element of the structure at a time is damaged.

### 3. Numerical example

We consider a 9-element plane truss with steel elements having Young's modulus of  $E_0 = 200 \text{ GPa}$  at the reference temperature of  $20 \text{ }^\circ\text{C}$ , a cross-sectional area of  $A = 0.0025 \text{ m}^2$  and material density of  $\rho = 7850 \text{ kg/m}^3$  (see Figure 4). We build the truss FEM model, compute its modal frequencies with a standard eigenvalue analysis, and the resulting first modal frequencies read  $f_1 = 36.71$ ,  $f_2 = 78.91$ ,  $f_3 = 82.00$ ,  $f_4 = 145.97$ , and  $f_5 = 219.22 \text{ Hz}$ .

A temperature distribution  $T$  of one-year duration is built by considering seasonal, daily, and random fluctuations (see Fig. 5a). Ten samples per day are considered for a total of 3650 samples per year. The temperature effect on the structure is then introduced at the supports (elements 10 and 11) assuming a non-linear temperature-dependent Young modulus as [7]:

$$E(T) = E_0[1 - 0.005(T - 20)^{-0.01T} + 0.05 \text{ rand}[\mathcal{N}(0, 1)]] \quad (3)$$

The variation of Young's modulus of the supports for the different temperature samples is shown in Fig. 5b.

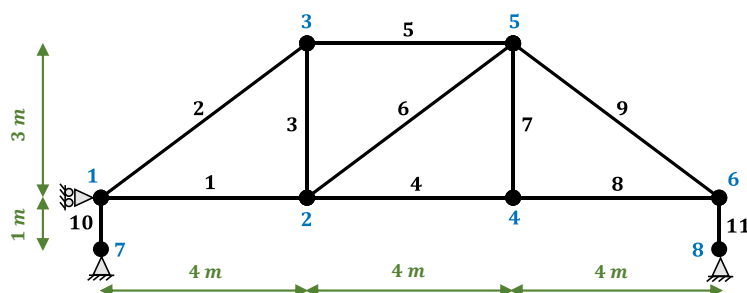


Figure 4. The truss under investigation.

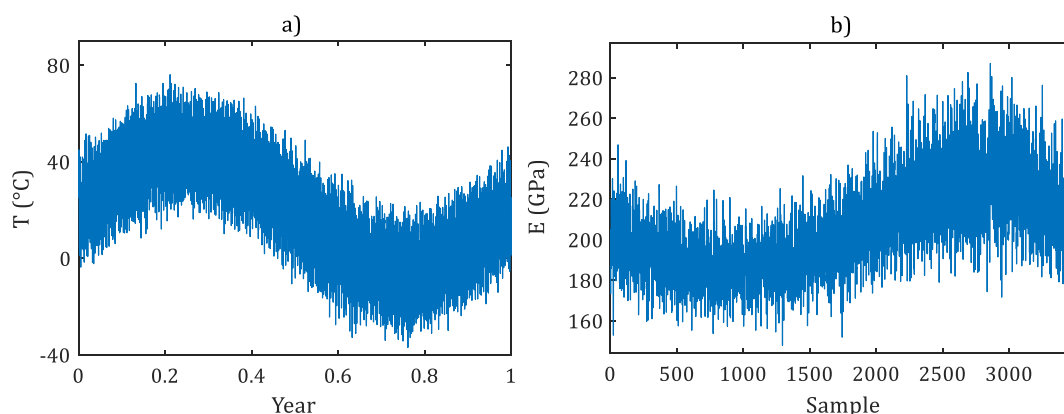
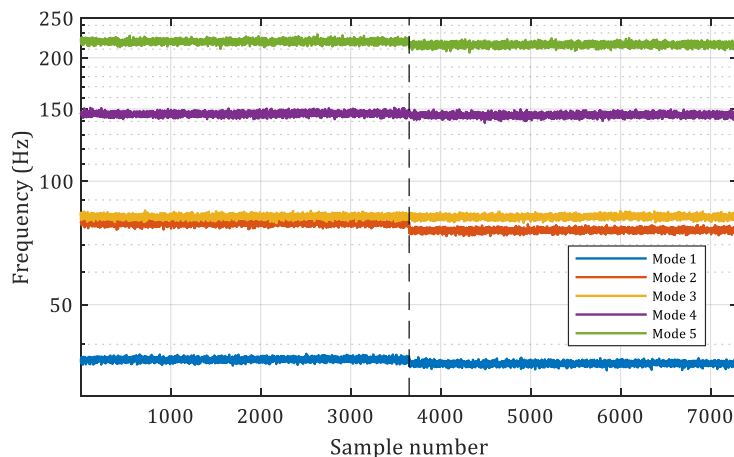


Figure 5. a) the simulated temperature variations for one year. b) the variations of support Young's modulus in one year using Eq. (3)

For the undamaged structure, the frequencies of vibration are computed for the 3650 temperature samples, namely over the entire first year. The first five frequencies are later contaminated by 1% of noise, as commonly observed in vibration-based SHM systems, and used

to set the baseline matrix  $\mathbf{HF}$ . These frequencies are represented in Fig. 6, i.e., the first 3650 samples. Using this set of frequencies, the 3650 DIs for the baseline are calculated utilizing the Mahalanobis distance. For this baseline, the DI value for a  $PFA = 0.05$ , the alarm threshold, corresponds to a  $\tau = 3.3084$  (see Fig. 7).



**Figure 6.** Pseudo frequencies of the healthy (first year) and the damaged (second year) structure for damage  $\kappa = 0.16$  on element 1.

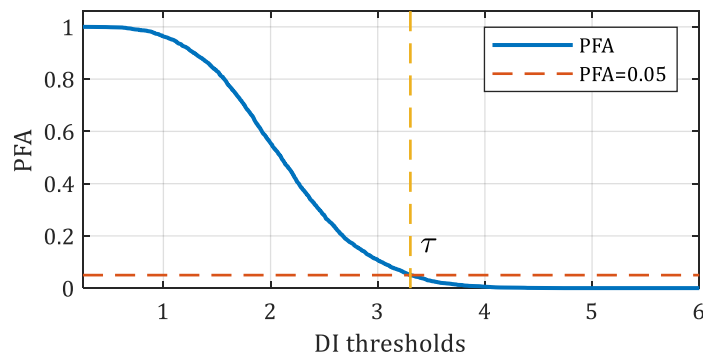


**Figure 7.** Variation of PFA with respect to the DI threshold ( $\tau$ ).

Similarly, for a given element  $i$  of the truss structure with damage size  $\kappa$ , the first five frequencies of vibration are computed for the 3650 temperature samples. This step is repeated for  $\kappa = 0.01$  to  $\kappa = 1$  with an increment of  $\kappa = 0.01$ . As an example in Fig. 6, the samples 3651 to 7300, show the first five pseudo-frequencies for damage size  $\kappa = 0.16$  in element 1. Damage  $\kappa = 0.16$  means that the element has lost 16% of its axial stiffness, for instance, due to a 16% reduction of its cross-section. For each  $\kappa$  value, the  $POD(\tau)$  is computed considering the 3650 DI samples, and the curve  $POD(\tau)$  vs  $\kappa$  is built. The value of  $\kappa$  for which the  $POD(\tau)$  reaches 0.95 is considered the minimum detectable damage for the element  $i$ , namely the  $MDD(i)$ . For instance, Fig. 8 shows the  $POD(\tau)$  vs  $\kappa$  for element 1, for which  $MDD(1)$  (the purple vertical line) is equal to 0.16.

Repeating the procedure for all the other truss elements  $i = 1, 2, \dots, 9$  allows computing the  $MDD$  for each element of the considered truss structure. The estimated  $MDDs$  are illustrated in



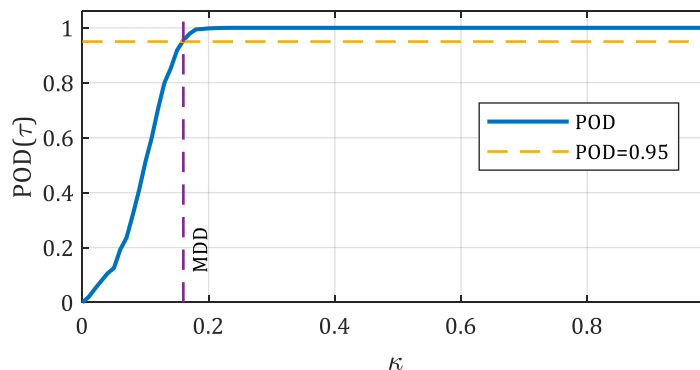


**Figure 8.** The variations of  $POD(\tau)$  with respect to different damage sizes on element 1 ( $\kappa$ ).

Fig. 9 for two different noise levels of 1% and 5%. It can be seen that the noise level noticeably increases the MDD.

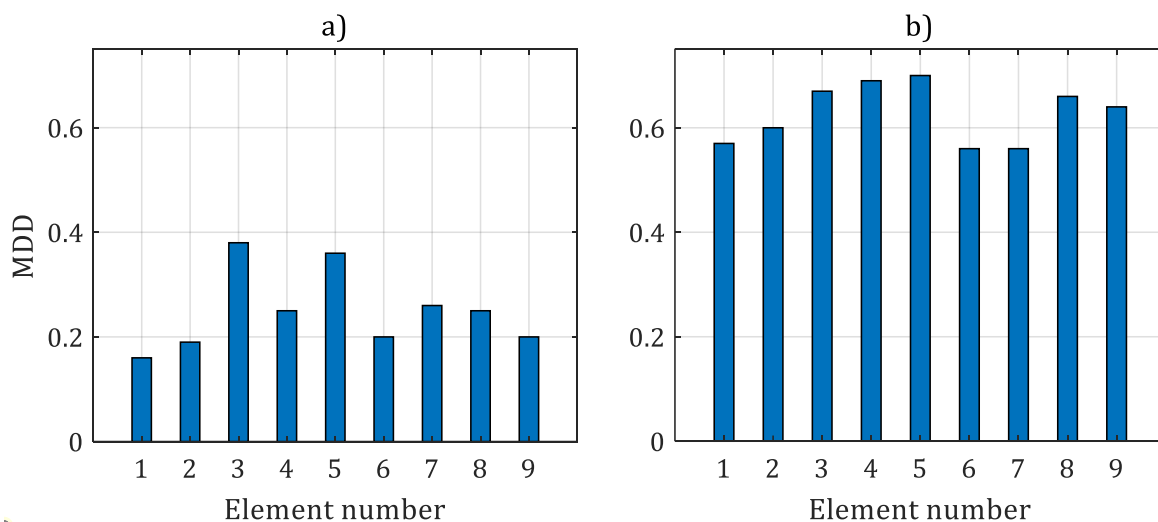


**Figure 9.** The minimum detectable damage (MDD) for different elements of the truss structure estimated by using the first five frequencies and a noise level of a) 1% and b) 5%.

### Conclusion

The present study introduces a methodology for selecting the alarm threshold in structural health monitoring systems based on the probability of false alarm and allows estimating the minimum detectable damage in a supervised framework. The proposed approach provides enhanced control over (i) the number of false alarms based on the owner’s budget and (ii) the risk tolerance by estimating the minimum detectable damage with a desired probability of detection. The methodology has been discussed through a numerical example, a steel truss, considering damage scenarios where only one element at a time is damaged. Still, the procedure can easily consider damage scenarios with multiple damaged elements, and it is not limited to truss structures. The results of the numerical example have demonstrated that the proposed approach can effectively set the alarm threshold based on the PFA, which in turn determines the number of false alarms generated by the SHM system. Additionally, the approach can estimate

the minimum detectable damage size, providing insight into the reliability of the SHM system for different damage scenarios. Overall, the proposed methodology can be used as a simple tool to compute effective DI for vibration-based SHM systems, minimizing the risk of having undetected damages.

### Acknowledgements

The presented work has been partially supported by the project “DS2: Digital Smart Structures”, funded by INAIL (National Institute for Insurance against Accidents at Work), BRIC 2021.

### References

- [1] Z. He, W. Li, H. Salehi, H. Zhang, H. Zhou, P. Jiao, Integrated structural health monitoring in bridge engineering, *Automation in Construction* 136 (2022) 104168.
- [2] R. Brincker, C. Ventura, Introduction to operational modal analysis, John Wiley & Sons, 2015.
- [3] A.-M. Yan, G. Kerschen, P. De Boe, J.-C. Golinval, Structural damage diagnosis under varying environmental conditions—part i: A linear analysis, *Mechanical Systems and Signal Processing* 19 (4) (2005) 847–864.
- [4] H. Sarmadi, A. Karamodin, A novel anomaly detection method based on adaptive mahalanobis-squared distance and one-class knn rule for structural health monitoring under environmental effects, *Mechanical systems and signal processing* 140 (2020) 106495.
- [5] C. Rainieri, G. Fabbrocino, Operational modal analysis of civil engineering structures, Springer, New York 142 (2014) 143.
- [6] A. Kita, N. Cavalagli, F. Ubertini, Temperature effects on static and dynamic behavior of consoli palace in gubbio, italy, *Mechanical Systems and Signal Processing* 120 (2019) 180–202.
- [7] M. Seif, L. Choe, J. Gross, W. E. Luecke, J. A. Main, D. McColskey, F. Sadek, J. M. Weigand, C. Zhang, Temperature-dependent material modeling for structural steels: formulation and application, US Department of Commerce, National Institute of Standards and Technology, 2016.
- [8] M. A. Wahab, G. De Roeck, Effect of temperature on dynamic system parameters of a highway bridge, *Structural Engineering International* 7 (4) (1997) 266–270.
- [9] X. Hua, Y. Ni, J. Ko, K. Wong, Modeling of temperature–frequency correlation using combined principal component analysis and support vector regression technique, *Journal of Computing in Civil Engineering* 21 (2) (2007) 122–135.
- [10] H. Zhou, Y. Ni, J. Ko, Structural damage alarming using auto-associative neural network technique: Exploration of environment-tolerant capacity and setup of alarming threshold, *Mechanical Systems and Signal Processing* 25 (5) (2011) 1508–1526.
- [11] Y. Ni, Y. Wang, C. Zhang, A bayesian approach for condition assessment and damage alarm of bridge expansion joints using long-term structural health monitoring data, *Engineering Structures* 212 (2020) 110520.
- [12] F. Falcetelli, N. Yue, R. Di Sante, D. Zarouchas, Probability of detection, localization, and sizing: The evolution of reliability metrics in structural health monitoring, *Structural Health Monitoring* 21 (6) (2022) 2990–3017.
- [13] M. Jahangiri, A. Palermo, S. Kamali, M. A. Hadianfard, A. Marzani, A procedure to estimate the minimum observable damage in truss structures using vibration-based structural health monitoring systems, *Probabilistic Engineering Mechanics* 73 (2023) 103451.
- [14] Y. Xia, B. Chen, S. Weng, Y.-Q. Ni, Y.-L. Xu, Temperature effect on vibration properties of civil structures: a literature review and case studies, *Journal of civil structural health monitoring* 2 (1) (2012) 29–46.